A Comparative Study of a Robust Multivariable and Monovariable H_∞ Controllers for Speed and direct current regulation of a Permanent Magnet Synchronous Machine Powered by an Inverter Voltage

J. KHEDRI[1] M. CHAABANE[1], M.SOUISSI[1]

[1]Laboratory of Sciences and Techniques of Automatic Control and Computer Engineering (Lab-STA), National School of Engineering of Sfax, University of Sfax, Postal Box 1173, 3038 Sfax, Tunisia

khedrijamel@yahoo.fr

Abstract: *For permanent magnet synchronous machine (PMSM), nonlinearity of its state model, external disturbances as well as parameters variations due to temperature and excessive use… make difficult the application of conventional methods. Thus the uses of a linear model and along with simplifying assumptions are necessary. The main purpose of such control law is to ensure stabilization and some performance criteria such that trajectory tracking and time specifications (response time, static error, overshoot…). In this paper a comparative study of a robust multivariable and monovariable H_∞ controllers for the speed and the direct current regulation of a permanent magnet synchronous machine is carried out. Both controllers are implemented under variations of ±10% of machine parameters and weighting filters integration. Experimental results are illustrated to prove the effectiveness of the comparative study.*

Key words: *Multivariable H_∞ controller, Monovariable H_∞ controller, Uncertainties, PMSM, Robust performance.*

1. INTRODUCTION

PMSMs are frequently used in low to mid power high performance industrial application such as robotics adjustable speed drives, computer peripheral, embedded systems and traction motor systems [1-2]. With the progress in magnetic power device, computer technologies, control theories and advances in the permanent Magnet motor market, the use of simulation tools is necessary for analyzing machine features. PMSM celebrity during recent years is due to its various ranges of applications awing to many important characteristics. It provides high efficiency, high power density, weight reduction and small size [3]. These advantages do not hide major disadvantages. Indeed the PMSM model is nonlinear and strongly coupled which leads to an uncertain PMSM model under parameters variations. Several works have been performed to deal with uncertainties. Authors of paper [4] have developed a method for the optimal control of a positioning drive with a permanent magnet synchronous motor in order to reduce or eliminate the influence of disturbances on the system dynamics. In papers [5] and [6], an adaptive control scheme based on reference model adaptive control approach is presented in the goal to compensate system parameters variations such as torque constant and inertia. In paper [7], the problem of control associated with brushless DC motors for direct-drive robotic application is presented. In this paper, the effects of magnetic saturation and reluctance variations are considered and a robust control law is developed to guarantee high performance of the system under uncertainties. Authors of paper [8-9] discuss the design of H_2 and H_∞ controllers for a permanent magnet synchronous machine drive system where disturbance rejection and transient response are investigated. In the presented study, a robust control law of current and speed regulation of a PMSM powered by an inverter voltage has been developed using a comparison of multivariable and monovariable H_∞ controllers. These kinds of controllers are insensitive to parameters variations which motivates us to develop such control laws.

The paper is organized as follows: in section 2, state space model of the PMSM and problem formulation are presented. In section 3, a robust monovariable H_∞ controller is computed by the

resolution of a special inequality and the guarantees of desired performances. Besides experimental results are presented. Section 4, is reserved to results given by the synthesis of a robust multivariable H_∞ controller supported by a comparison of performances derived from the two controllers and those given by a PI one.

2. STATE SPACE MODEL OF THE PMSM AND PROBLEM STATEMENT

a. STATE SPACE MODEL OF THE PMSM

To obtain a simple and detailed state model which allows perfect simulation of the PMSM model on rotor reference frame, some simplifying hypotheses are used [8]. Thus the mathematical nominal model of the PMSM is given as follows [9]:

$$\begin{aligned}
\frac{dI_d}{dt} &= -\frac{R}{L_d}I_d + \frac{L_q}{L_d}w_r I_q + \frac{1}{L_d}v_d \\
\frac{dI_q}{dt} &= -\frac{R}{L_q}I_q - \frac{L_d}{L_q}w_r I_d - \frac{\emptyset}{L_q}w_r + \frac{1}{L_q}v_q \\
\frac{dw_r}{dt} &= p\frac{(c_e - c_r)}{J} - \frac{f_c}{J}w_r \\
c_e &= p\left[L_d - L_q\right]I_d + \emptyset]I_q \\
\frac{dw_r}{dt} &= \frac{p^2}{J}\left[L_d - L_q\right]I_d + \emptyset]I_q - \frac{f_c}{J}w_r - \frac{p}{J}c_r
\end{aligned} \tag{1}$$

Where

$v_{d\text{-}q}$: d-q axis stator voltages
$I_{d\text{-}q}$: d-q axis stator currents
$L_{d\text{-}q}$: d-q axis inductances
R: the stator resistance
$\emptyset$: the flux linkage of the permanent magnets
w_r: the rotor speed
f_c: the friction coefficient
J: the moment of inertia
$c_{e\text{-}r}$: the electromagnetic and the load torques
p: the number of pole.

The design of the two control laws is made around the nominal model which is derived from a linearization around an operating point (x^0, u^0) so that:

$$x^0 = [I_{d0} \quad I_{q0} \quad w_{r0}]^T, u^0 = [v_{d0} \quad v_{q0}]^T$$

The linearized nominal model will be written:

$$\begin{aligned}
\delta\dot{x} &= A\delta x + B\delta u + Dv \\
y &= C\delta x
\end{aligned} \tag{2}$$

Where

$$\delta x = [\delta I_d \quad \delta I_q \quad \delta w_r]^T, \delta u = [\delta v_d \quad \delta v_q]^T$$

$$A = \begin{bmatrix} -\frac{R}{L_d} & \frac{L_q}{L_d}w_{r0} & \frac{L_q}{L_d}I_{q0} \\ -\frac{L_d}{L_q}w_{r0} & -\frac{R}{L_d} & -\frac{\emptyset}{L_q} - \frac{L_d}{L_q}I_{d0} \\ \frac{p^2}{J}(L_d - L_q)I_{q0} & \frac{p^2}{J}[\emptyset + (L_d - L_q)I_{d0}] & -\frac{f_c}{J} \end{bmatrix}$$

$$B = \begin{bmatrix} \frac{1}{L_d} & 0 \\ 0 & \frac{1}{L_q} \\ 0 & 0 \end{bmatrix}, C = \begin{bmatrix} 1 & 0 & 0 \\ 0 & 0 & 1 \end{bmatrix}, D = \begin{bmatrix} 0 \\ 0 \\ -\frac{p}{J} \end{bmatrix}$$

b. PROBLEM STATEMENT

First of all, lets recall that the nominal state model of the PMSM can have a variation under some conditions such as excessive use and temperature. Parameters that often vary are those listed in the electrical and mechanical time constants denoted $\boldsymbol{\tau}_e$ and $\boldsymbol{\tau}_{mec}$ respectively. Indeed the stator resistance R may vary by temperature and the moment of inertia J can change after a long use which generally leads to its increase. Taking in consideration these variations, all uncertainties in the model can be gathered in an output multiplicative uncertainty form as illustrated in Figure (1)

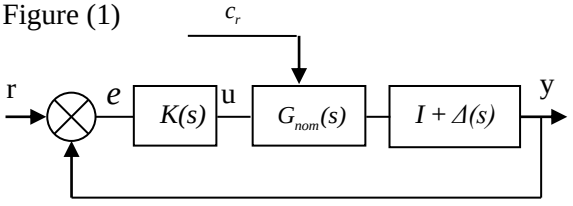

Fig. 1.Feedback uncertain configuration

In this configuration, $G_{nom}(s)$ define the nominal model.

r is a reference signal which refers in our study to the current I_{dref} or the speed w_{ref}.
Δ represents the deviation of variations of the nominal parameters of the machine which is equal to ±10% of each value.

c_r is the load torque which represents the external disturbance. As cited above, we assume that uncertain parameters are the subject of a variation of ±10% of all machine parameters from their nominal values and we adopt the following uncertain plans:

Case 1:

$$(R)_{nom} + \Delta(R)_{nom}$$
$$(L_q)_{nom} + \Delta(L_q)_{nom}, (\emptyset)_{nom} + \Delta(\emptyset)_{nom}$$
$$(J)_{nom} + \Delta(J)_{nom}, (f_c)_{nom} + \Delta(f_c)_{nom}$$

Case 2:

$$(R)_{nom} + \Delta(R)_{nom}$$
$$(L_q)_{nom} - \Delta(L_q)_{nom}, (\emptyset)_{nom} - \Delta(\emptyset)_{nom}$$
$$(J)_{nom} + \Delta(J)_{nom}, (f_c)_{nom} - \Delta(f_c)_{nom}$$

Case 3:

$$(R)_{nom}, (L_q)_{nom} - \Delta(L_q)_{nom}$$
$$(\emptyset)_{nom} + \Delta(\emptyset)_{nom}, (J)_{nom}$$
$$(f_c)_{nom} - \Delta(f_c)_{nom}$$

Case 4:

$$(R)_{nom} + \Delta(R)_{nom}$$
$$(L_q)_{nom} - \Delta(L_q)_{nom}, (\emptyset)_{nom} + \Delta(\emptyset)_{nom}$$
$$(J)_{nom} + \Delta(J)_{nom}, (f_c)_{nom}$$

We give below the frequency response of the nominal system and those uncertain

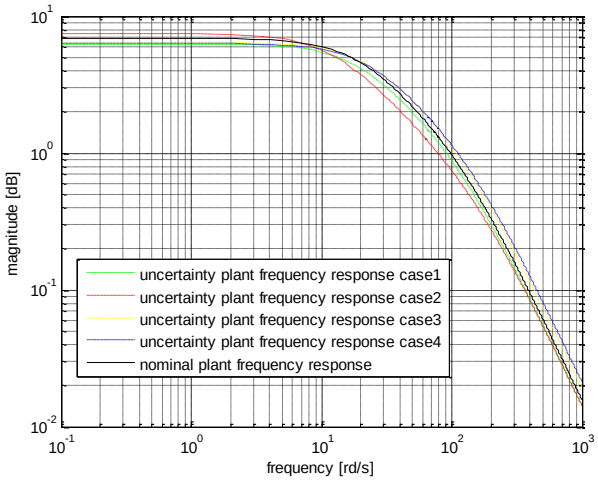

Fig. 2. Frequency responses of the nominal and uncertain plants

Let's consider then the generalized feedback system as shown in Figure (3) where the state space representation is adopted to solve this standard problem known as H_∞ loop-shaping. The objective of this methodology is to formulate frequency domain performances as H_∞ constraints [10].

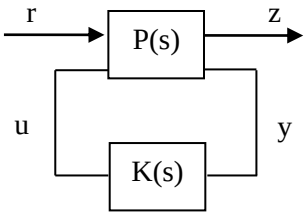

Fig. 3. Generalized plant and controller configuration

Based on this standard block diagram, we can derive the following equation:

$$\begin{bmatrix} z \\ y \end{bmatrix} = P \begin{bmatrix} r \\ u \end{bmatrix} = \begin{bmatrix} P_{11} & P_{12} \\ P_{21} & P_{22} \end{bmatrix} \begin{bmatrix} r \\ u \end{bmatrix} \quad (3)$$

u is the controlled input, *r* is the external disturbance input, *y* is the measured variable and *z* is the adjustable robust output that we need to evaluate system performance.

P is the augmented plant that contains weighting functions which characterize robust performance and uncertain system.

K is the output feedback controller to design so that the closed-loop transfer function matrix $F(P(s), K(s))$ is stable and its H_∞ norm is less than a positive constant γ:

$$F(P(s), K(s)) \text{ stable}$$
$$\|F(P(s), K(s))\|_\infty < \gamma \quad (4)$$

Notice: γ refers to desired performance level of the closed-loop system which is the ratio between *z* and *r*.

In order to ensure this condition, three weight functions are added to the plant as shown in Figure (4). Indeed the error ε is weighted by the weight function W_s called the tracking performance. The command u is weighted by W_u known as the robust performance and the output *y* is weighted by W_T .

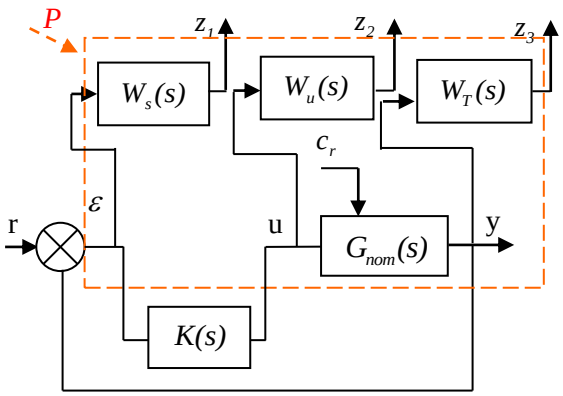

Fig. 4. Feedback uncertain configuration with weighting functions

$$z_1(s) = W_s(s)S(s)r(s)$$
$$z_2(s) = W_u(s)K(s)S(s)r(s) \quad (5)$$
$$z_3(s) = W_T(s)T(s)r(s)$$

Here

$S(s) = \frac{1}{1+G_{nom}(s)K(s)}$ is the sensitivity function and $T(s) = \frac{K(s)G_{nom}(s)}{1+G_{nom}(s)K(s)}$ is the complementary sensitivity function.

If we set $z = [z_1 \quad z_1 \quad z_1]^T$ it is easy to derive that:

$$\begin{bmatrix} z \\ e \end{bmatrix} = P(s)\begin{bmatrix} r \\ u \end{bmatrix} = \begin{bmatrix} P_{11}(s) & P_{12}(s) \\ P_{21}(s) & P_{22}(s) \end{bmatrix}\begin{bmatrix} r \\ u \end{bmatrix} \quad (6)$$

Where

$$P_{11}(s)\begin{bmatrix} W_s \\ 0 \\ 0 \end{bmatrix}, P_{12}(s)\begin{bmatrix} -W_sG_{nom}(s) \\ W_u \\ W_TG_{nom}(s) \end{bmatrix}$$
$$P_{21}(s) = I, P_{22}(s) = -G_{nom}(s)$$

We have then

$$z(s) = \begin{bmatrix} z_1(s) \\ z_2(s) \\ z_3(s) \end{bmatrix} = \begin{bmatrix} W_s(s)e(s) \\ W_u(s)u(s) \\ W_T(s)y(s) \end{bmatrix} = \begin{bmatrix} W_s(s)S(s) \\ W_u(s)K(s)S(s) \\ W_T(s)T(s) \end{bmatrix} r(s) \quad (7)$$

According to condition (4), the H_∞ control objective is to design a stabilized controller *K(s)* in the way that the closed-loop system is stable and the H_∞ norm of z is less than γ:

$$\|z(s)\|_\infty < \gamma \quad (8)$$

The sensitivity function *S(s)* is considered as a high-pass filter in order to reduce the tracking error ε Then to shape *S(s)*, the weighting filter $W_s(s)$ is considered as a low-pass filter of the form:

$$W_s(s) = \frac{ks+\omega}{s+b\omega} \quad (9)$$

k is the high frequency disturbance gain, ω is the crossover frequency and *b* is the gain of control signal in low frequency gain.

For the weighting filter $W_u(s)$, since it acts on the transfer $K(s)S(s)$, it is chosen as a scalar value λ in order to reduce the order of the controller $K(s)$ and limit its complexity.

The weighting function $W_T(s)$ is chosen to adjust uncertainties norm that the closed-loop system must allow [11-12]. Thus it is selected as a high-pass filter in order to shape the complementary sensitivity *T(s)* which is considered as a low-pass filter:

$$W_T(s) = \frac{as+b_1}{cs+d} \quad (10)$$

Where a, b_1, c and d, are constants.

An efficient method that leads to the design of these parameters introduced in each weighting functions, for all robustness and performances criteria for the design of the H_∞ controller, is summarized in the flowchart below.

In this flowchart, the selection of such weighting function is in the relation with the guarantee of robustness and performance specifications. Thus values a, b_1, c, d, k, b and λ are adjusted (incremented or decremented) in such a way that each step of the flowchart is satisfied until the controller is retained. In the next section, we will give shapes of these different functions.

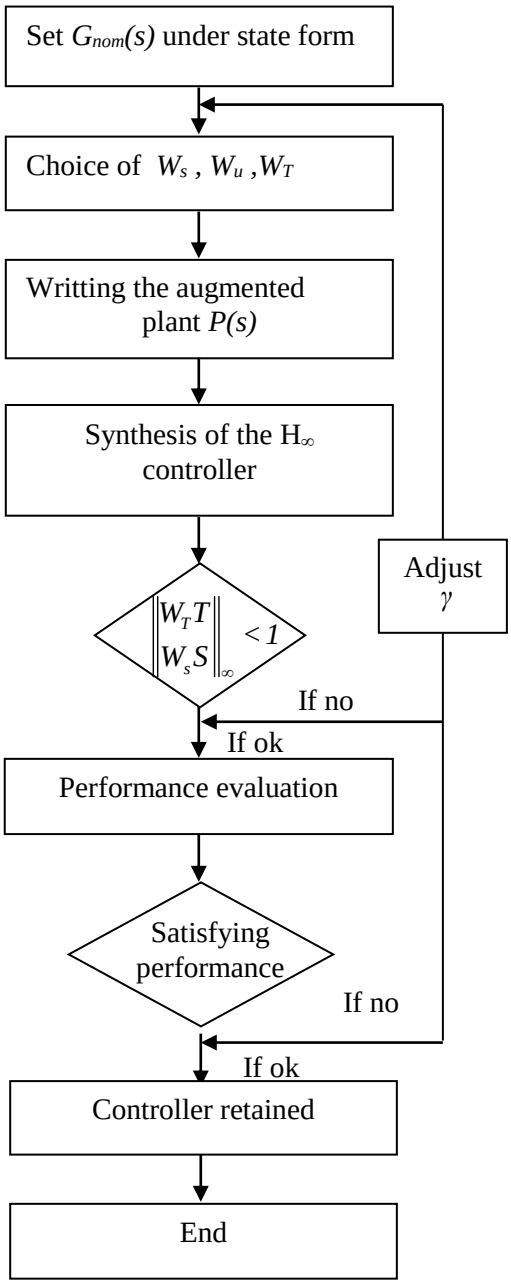

3. MONOVARIABLE H∞ STRUCTURE

Monovariable H∞ structure, illustrated in Figure (7), consists of a H∞ controller for the speed w_r and a PI regulator for the current which is regulated to zero. This choice ($I_d = 0$) is in order to allow the PMSM to function in oriented flux and to ensure a perfect decoupling machine model because of the great coupling between the two axes d and q. Thus in our study, in order to control the speed w_r and the direct current I_d we have adopted the following nominal transfer diagonal matrix H which includes open-loop transfer functions of variable that we aim to control $H_{Idnom}(s)$ and $H_{wrnom}(s)$:

$$H = \begin{bmatrix} H_{Idnom}(s) & 0 \\ 0 & H_{wrnom}(s) \end{bmatrix} \quad (11)$$

Here

$$H_{Idnom}(s) = \frac{1}{R + L_d s}$$

$$H_{wrnom}(s) = \frac{\frac{p^2 \emptyset}{JL_q}}{s^2 + \frac{L_q f_c + JR}{p^2 \emptyset} s + \frac{R f_c + p^2 \emptyset^2}{p^2 \emptyset}}$$

Notice: H is chosen diagonal to ensure full decoupling.

In our study and as mentioned in the section 2, we assume a variation of motor parameters from their nominal values of ±10%.

$W_s(s) = \frac{ks+\omega}{s+b\omega} = \frac{13.87s+1387.5}{s} = \frac{ks+\alpha}{s}$ in order to obtain for $\alpha = 1387.5$ a closed-loop response time of 77 ms as shown in Figure (6) and a short rise time and a minimal tracking error. Indeed α sets the rise time, the greater it is, the faster closed-loop response and the shorter rise time. $k = 13.87$ in order to obtain a module margin of at least 6dB for $W_s^{-1}(s)$.

$W_u(s) = 0.01$

$W_T(s) = \frac{0.1s+1}{7.84e-4s+0.1}$ in order to wrap all uncertainties as illustrated in Figure (5) .c) below:

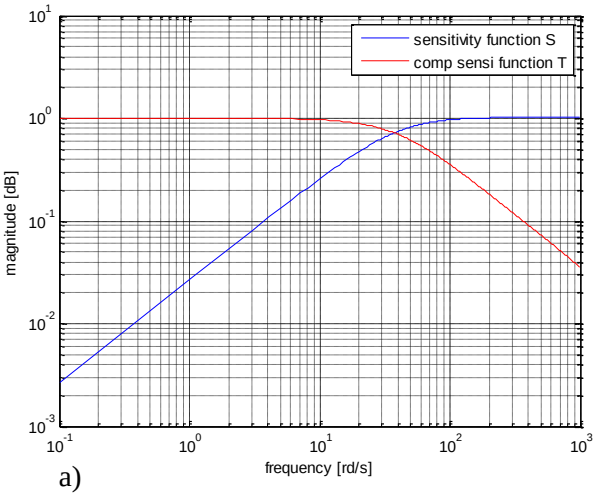

a)

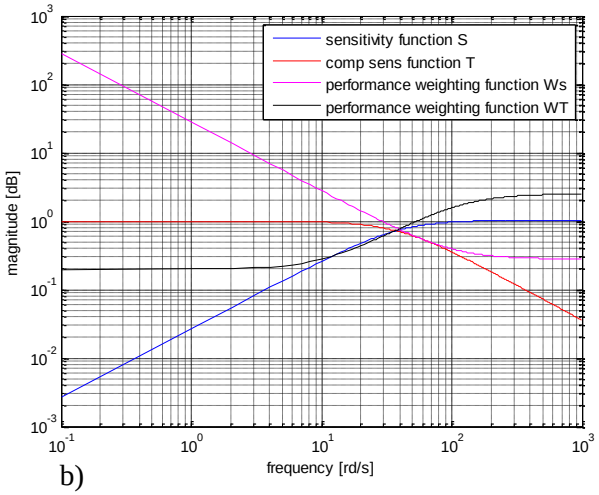

b)

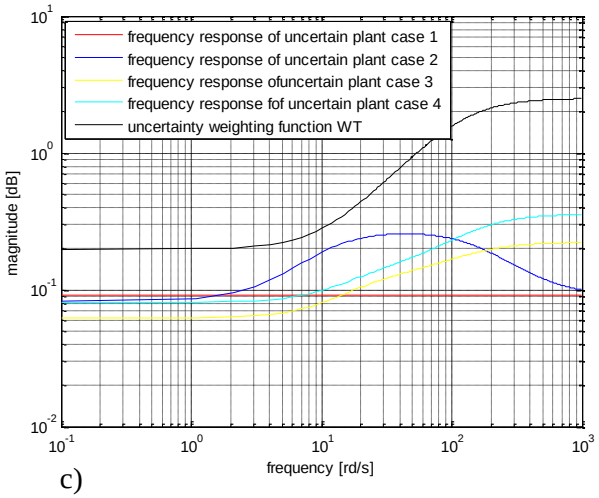

c)

Fig. 5. a) Closed-loop sensitivity and complementary sensitivity functions, b) performance weighting functions , c) uncertainties weighting functions under monovariable H_∞ controller

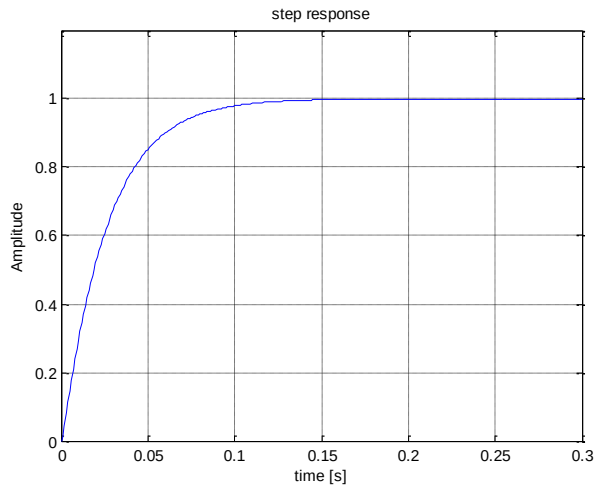

Fig. 6. Step response of the closed-loop system under monovariable H_∞ controller

The H_∞ controller K satisfying (4) and derived from the algorithm described above is given as follows:

$$K(s) = \frac{9308s^3 + 2.523e006s^2 + 1.916e008s + 2.702e009}{s^4 + 2990s^3 + 4.446e006s^2 + 4.948e008s - 1.031e-005} \qquad (12)$$

With the selected weighting functions, the control design algorithm gives a controller with desired performance γ=1.24218.

Experimental results are provided in the following figures according to the block scheme and the test benchmark presented in Figure (7) and (8) respectively.

These experimental results are derived from the use of a Dspace 1104 card, two identical coupled PMSM: one is used as a motor and the other (PMSG) coupled to the shaft of the main PMSM is used as a load. These PMSMs are fed by a two level voltage inverter. The control algorithm has been generated by the software Matlab/Simulink and converted to machine language via control desk software. Motors parameters are listed in table 1 as follows:

TABLE 1

Parameter of the PMSM

Machine power	1KW
Rated current	6.5A
Pole pair number (p)	2
d-axis inductance L_d	4.5mH
q-axis inductance L_q	4mH
Stator resistance R	0.56 Ω
Machine inertia J	$2.08.10^{-3}$Kg.m^2
Friction coefficient f_c	$3.9.10^{-3}$Nm.s.rad^{-1}
Magnet flux constant Ø	0.064wb

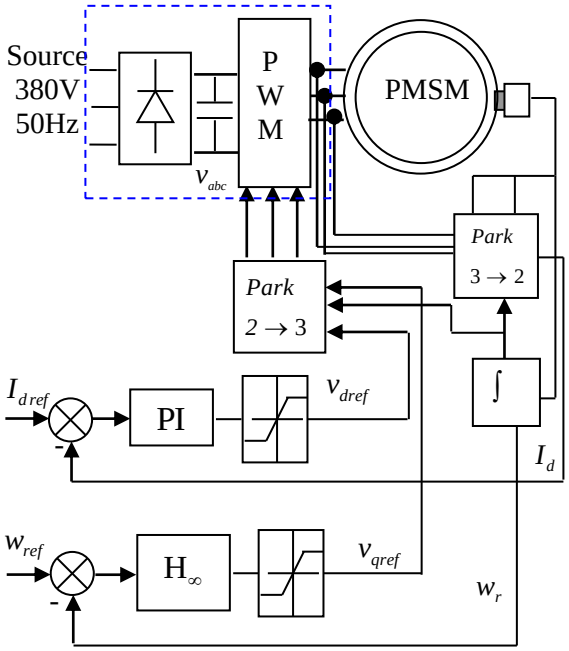

Fig. 7. Overall scheme of the monovariable H_∞ controller of the PMSM

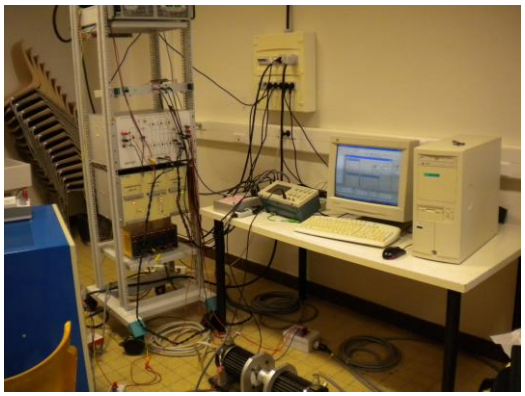

Fig.8. Photo of the test benchmark

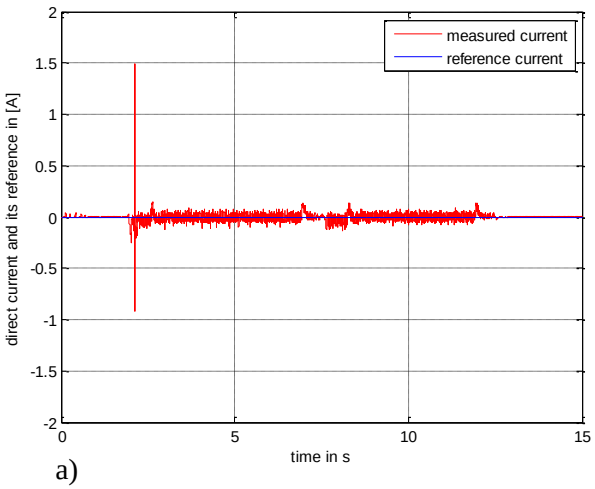

a)

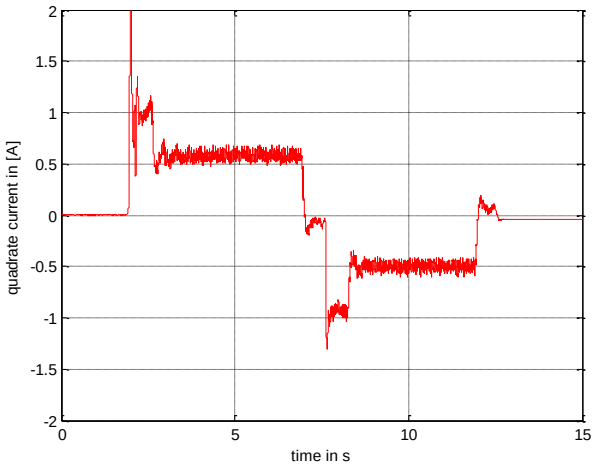

b)

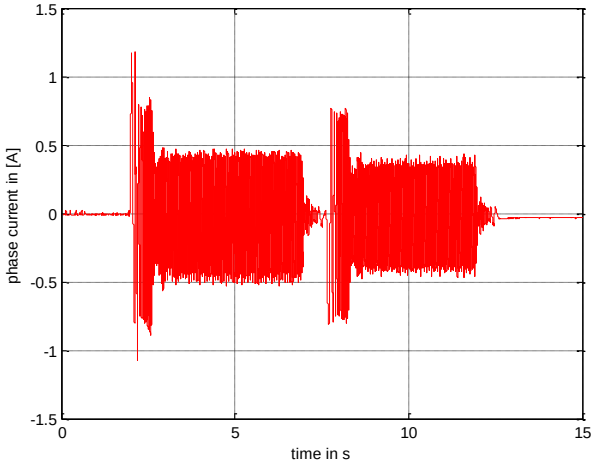

c)

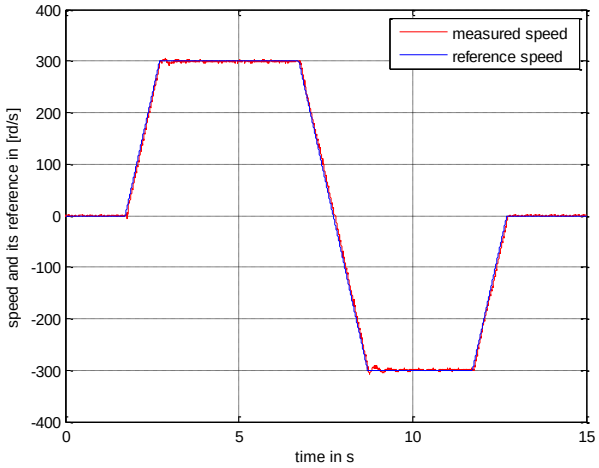

d)

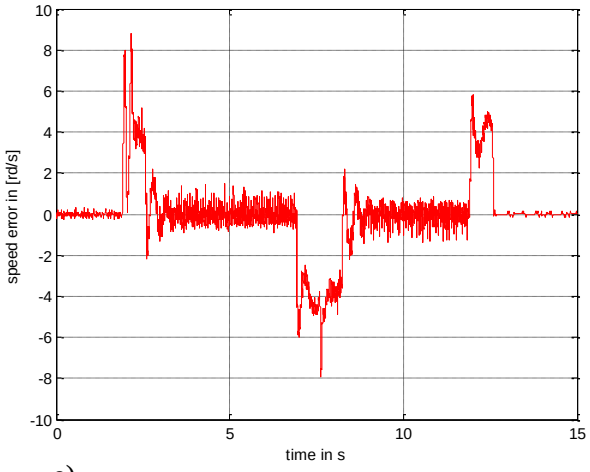

e)

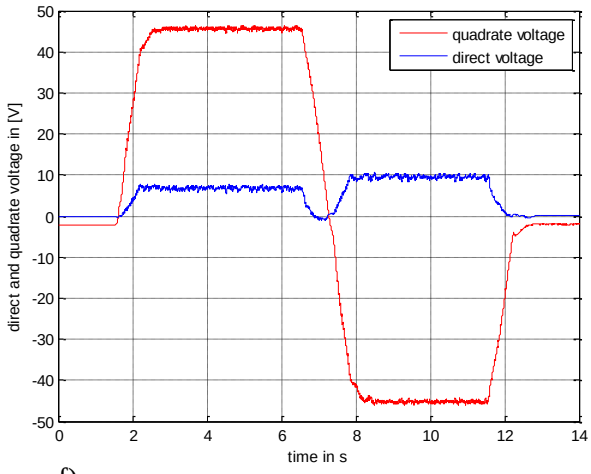

f)

Fig. 9. Experimental results under monovariable H_∞ controller without charge: a) I_d measured current, b) I_q measured current, c) phase current, d) measured speed e) tracking speed error, f) quadrate and direct voltages

These figures show results given by the synthesis of the monovariable H_∞ controller in presence of parameters variations and without load torque. According to these figures we can derive that the proposed method has good results. Indeed Figure (9) a) shows that the direct current I_d tracks well its reference. Figure (9).d) illustrate the measured speed which converges quickly to its trajectory with a moderate overshoot.

4. MULTIVARIABLE H_∞ STRUCTURE

The robust multivariable H_∞ controller is designed based on the configuration shown in Figure (3) and (4) of section 2. The objective is also the synthesis of a stabilized controller N such that the condition (4) is satisfied in which K is replaced by N.

The selection of the weighting filter matrix $W_s(s), W_u(s)$ and $W_T(s)$ is made in the same way as in the design of the monovariable H_∞ controller. The only difference is that previously, weighting filter matrix are of a first order view to the fact that variable which we desire to control (I_d and w_r) are controlled separately. Indeed the direct current I_d is regulated by a PI regulator while the speed w_r is controlled through the monovariable H_∞ controller.

In this section, we will apply the multivariable H_∞ controller for both mentioned variable and we will adopt the same nominal transfer diagonal matrix H. In this regard, weighting filter matrix $W_s(s)$, $W_u(s)$ and $W_T(s)$ are a 2x2 square diagonal matrix.

Of the same reasoning, $W_s(s)$ and $W_T(s)$ are chosen to be respectively low-pass and high-pass filters in order to ensure robustness and performance specifications:

$$\begin{aligned} W_s(s) &= \mathrm{diag}\left(\frac{ks+\omega}{s+\beta}, \frac{ks+\omega}{s+\beta}\right) \\ W_T(s) &= \mathrm{diag}\left(\frac{as+b}{cs+d}, \frac{as+b}{cs+d}\right) \\ W_u(s) &= \mathrm{diag}(\lambda, \lambda) \end{aligned} \quad (13)$$

As previously, all motor parameters are subject of a variation of ±10%. Thus for comparison purpose of the two controllers, (minimize the effect of disturbances, reduce the tracking error and obtain a module margin at least 6dB), $W_s(s)$ is chosen as follows:

$$W_s(s) = \begin{bmatrix} \frac{0.003659s+2.1522}{s} & 0 \\ 0 & \frac{0.003659s+2.1522}{s} \end{bmatrix} \quad (14)$$

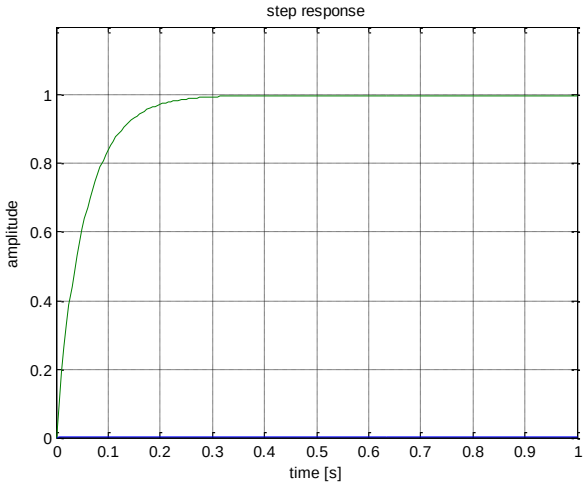

Fig. 10. Step response of the closed-loop system under multivariable H_∞ controller

To ensure robustness of the system against uncertainties $W_T(s)$ is set as follows:

$$W_T(s) = \begin{bmatrix} \frac{0.003s+1}{0.0068s+1} & 0 \\ 0 & \frac{0.003s+1}{0.0068s+1} \end{bmatrix} \quad (15)$$

With the intention of reducing the order of the controller $W_u(s)$ is given by:

$$W_u(s) = \begin{bmatrix} 0.01 & 0 \\ 0 & 0.01 \end{bmatrix} \quad (16)$$

Remark: parameters introduced in each weighting function, for all robustness and performances specifications for the design of the multivariable H_∞ controller, are selected based on the same procedure of the flowchart of the previous section.

Performances and robustness weighting function shapes are shown in Figure (11) below.

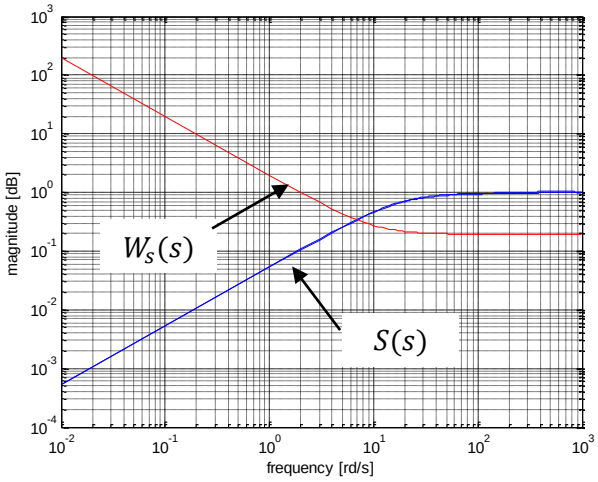

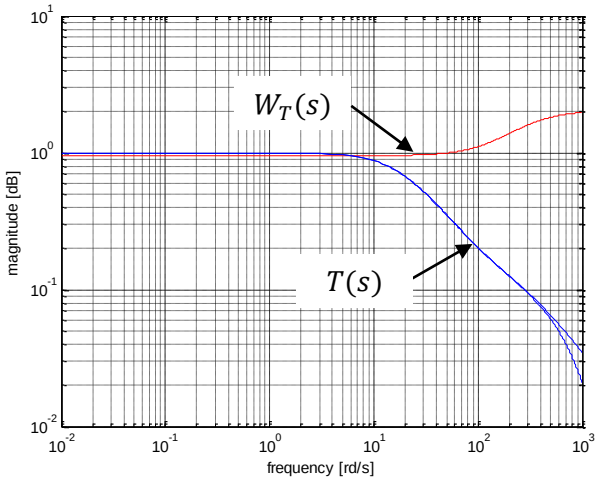

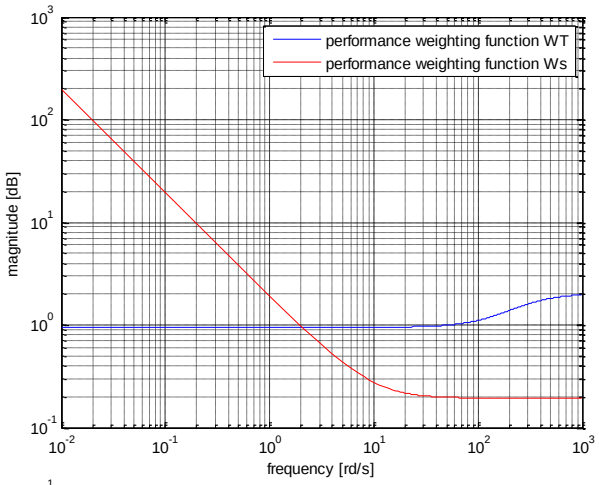

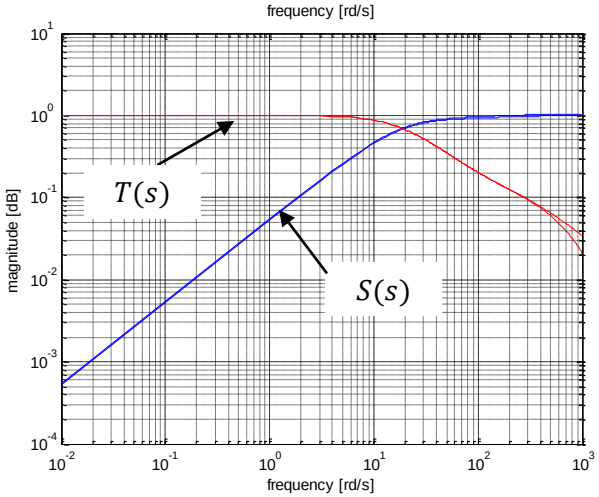

Fig. 11. Performance weighting functions under multivariable H_∞ controller

The multivariable H_∞ controller N and the desired performance γ satisfying (4) and derived from the algorithm described above are computed:

$$N(s) = \begin{bmatrix} N_{11}(s) & N_{12}(s) \\ N_{21}(s) & N_{22}(s) \end{bmatrix} \quad (17)$$

γ= 0.9453125

Where

$$N_{11}(s) = \frac{3.181e009s^4 + 1.095e012s^3 + 1.537e014s^2 + 7.513e015s - 1.99.1}{D(s)}$$

$$N_{12}(s) = \frac{-143.1s^6 + 1.016e006s^5 + 1.725e009s^4 + 1.388e012s^3 + 3.752e014s^2 + 2.966e016s - 1905}{D(s)}$$

$$N_{21}(s) = \frac{-138.7s^6 - 1.016e006s^5 - 1.17e010s^4 + 4.624e012s^3 - 4.263e014s^2 - 7.7353e014s - 1099}{D(s)}$$

$$N_{22}(s) = \frac{1910s^6 + 2.36e007s^5 + 1.257e010s^4 + 2.216e012s^3 + 1.417e014s^2 + 1.908e015s + 7844}{D(s)}$$

$$D(s) = s^7 + 1.369e004s^6 + 2.425e007s^5 + 2.012e010s^4 + 6.492e012s^3 + 6.926e014s^2 - 624.9s - 3.515e - 11$$

Experimental results are provided in the following figures according to the test benchmark described in section 3 and the block scheme presented in Figure (12)

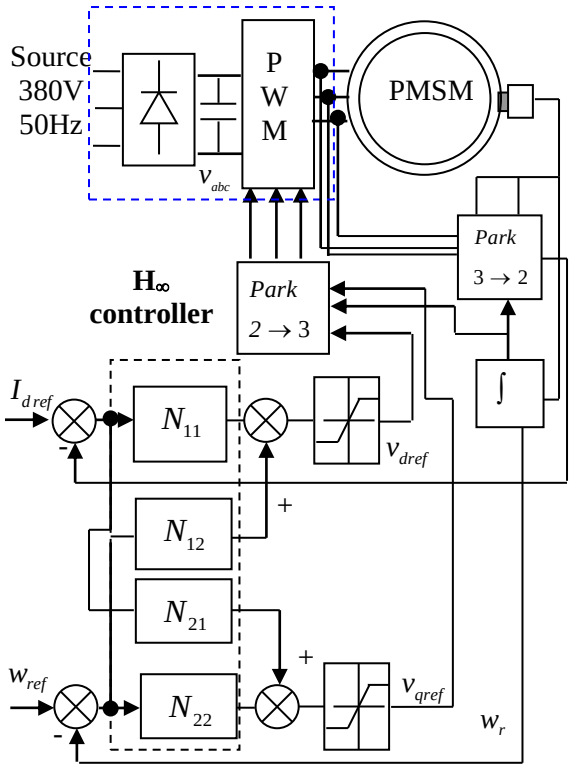

Fig. 12. Overall scheme of the multivariable H∞ controller of the PMSM

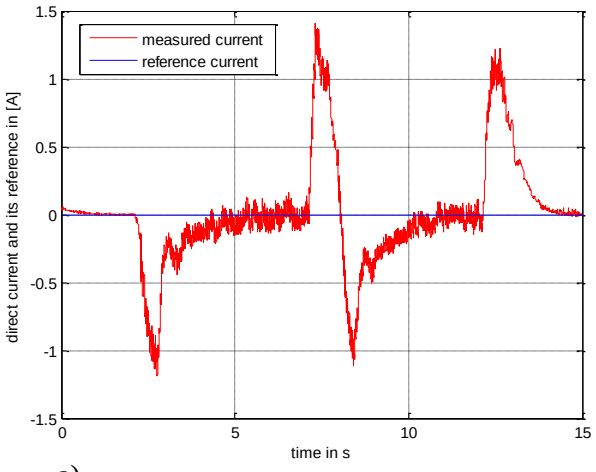

a)

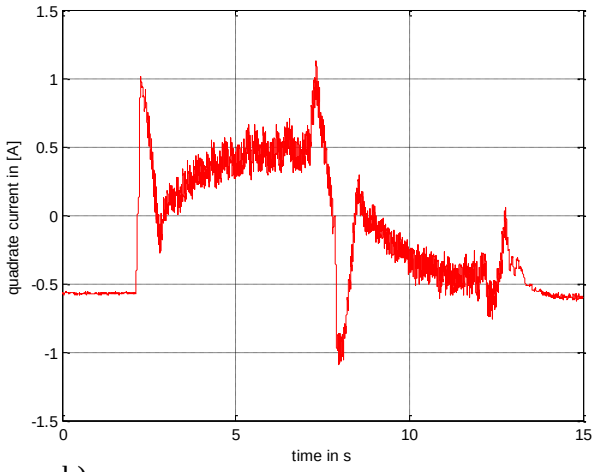

b)

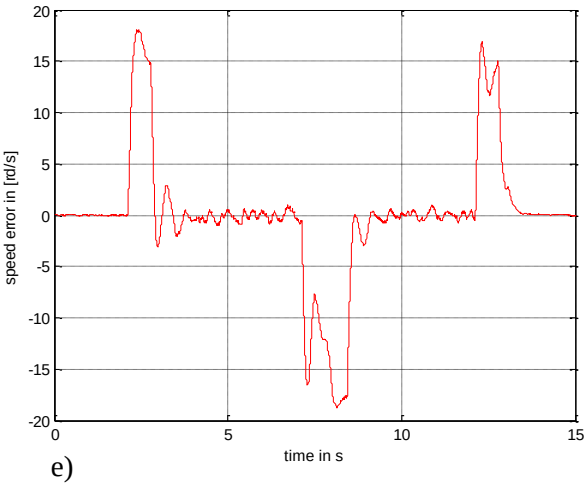

e)

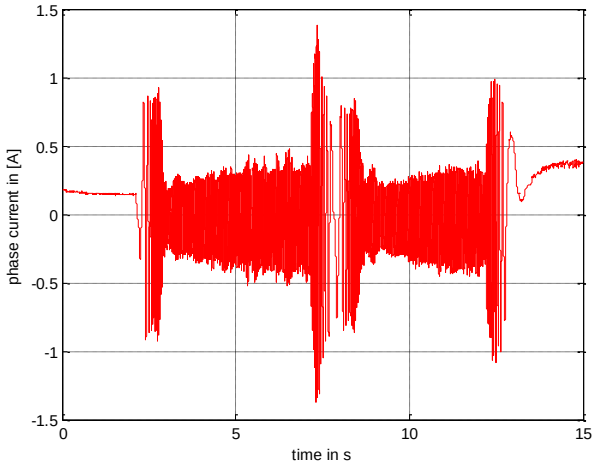

c)

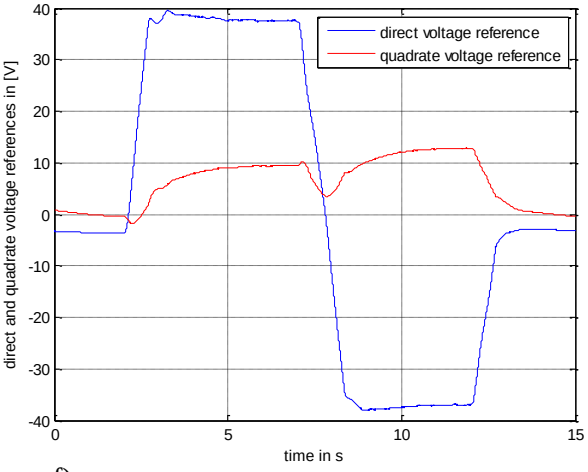

f)

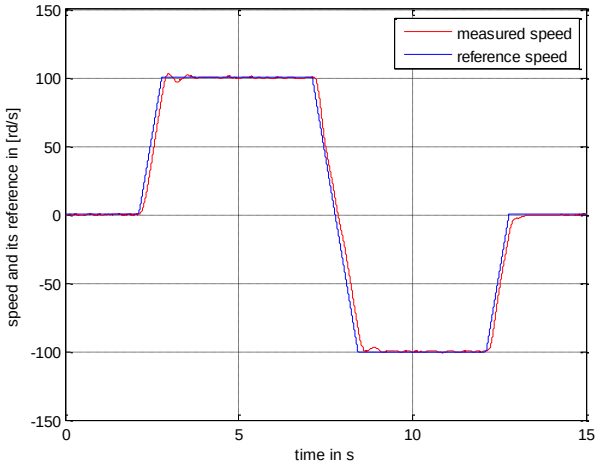

d)

Fig. 13. Experimental results under multivariable H_∞ controller: a) I_d measured current, b) I_q measured current, c) phase current, d) measured speed, e) tracking speed error, f) quadrate and direct voltages

These figures illustrate results given by the synthesis of the multivariable H_∞ controller under parameters variations and without load torque. Referring to these figures we can note that the proposed method has satisfactory results in terms of trajectory tracking. But the disadvantage of this control law is its high order, besides in transitory regime; there are important current peaks in regard with the monovariable H_∞ controller

A comparison of results given by the two controllers is summarized in table 2. According to the results listed in this table, we can conclude that

the monovariable H_∞ controller achieves the fastest response time and the smallest training gap and overshoot. However static errors of the two controllers are very close.

In order to prove further robustness of the monovariable H_∞ controller in comparison of a PI control law, we are allowed to present some experimental results of the two controllers under and without load torque.

Notice: the structure and different steps of the PI controller's synthesis for current and speed are based on the method of pole placement as detailed in [13-14].

For currents loops, $K_p = 5.9$, $K_i = 723$,in the purpose to perform a prescribed settling time of 0.24s.

For the speed, $K_p = 0.09$, $K_i = 0.168$ which are derived from depreciation coefficient fixed at 0.707, and a natural pulsation at 17 rd/s. This choice is done in order to obtain a closed-loop system response with a moderate overshoot 5.8 % and a little time response of 0.22s.
The direct current I_d is regulated to zero

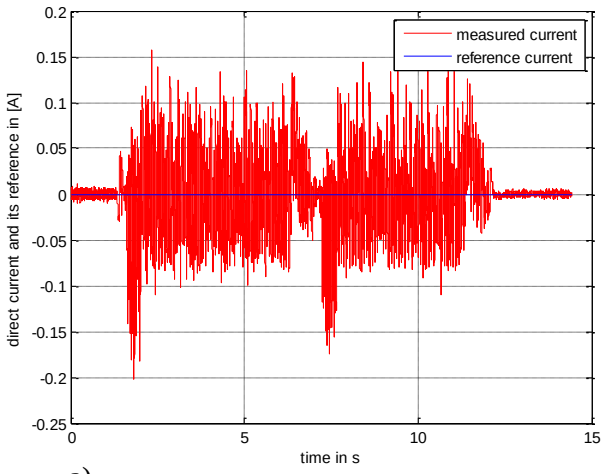

a)

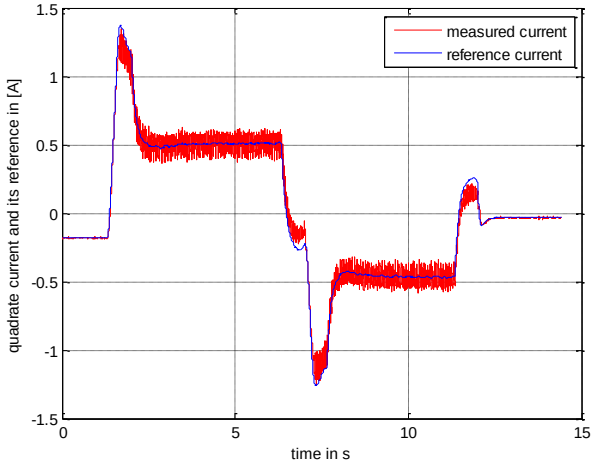

b)

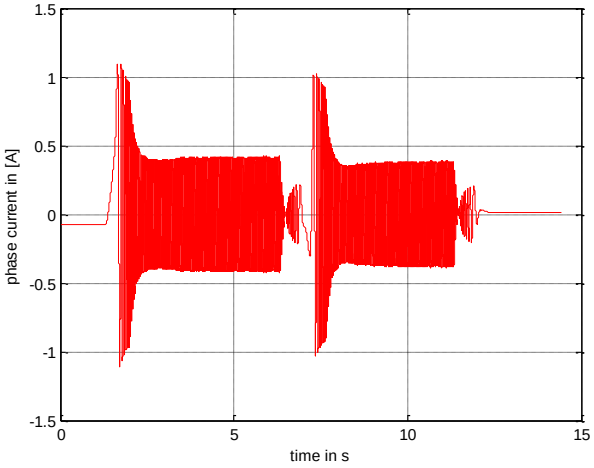

c)

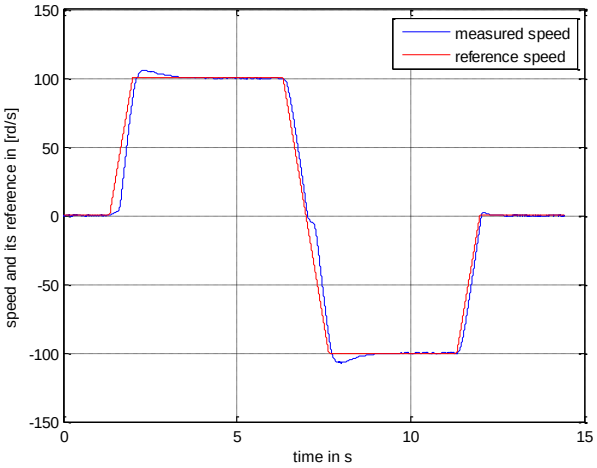

d)

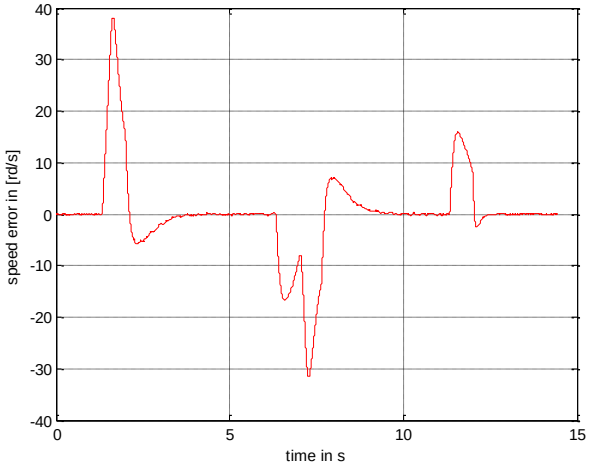

e)

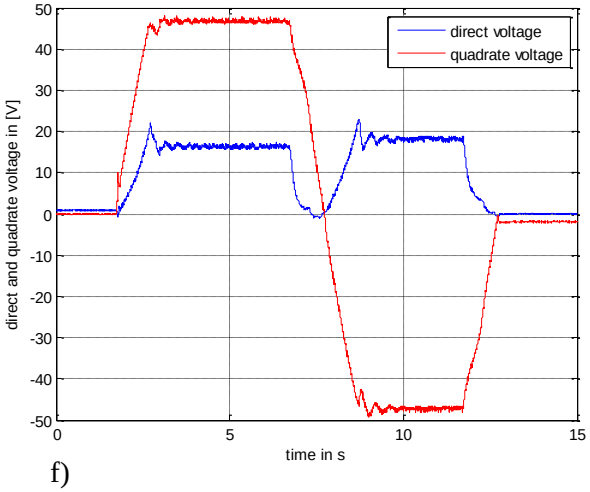

f)

Fig. 14. Experimental results under PI controller without charge: a) I_d measured current, b) I_q measured current, c) phase current, d) measured speed e) tracking speed error, f) quadrate and direct voltage

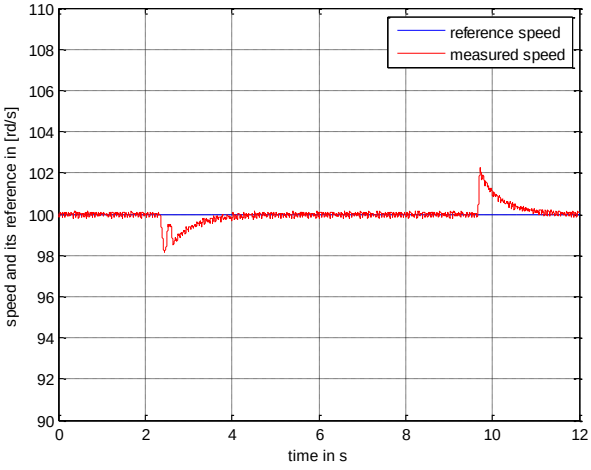

b)

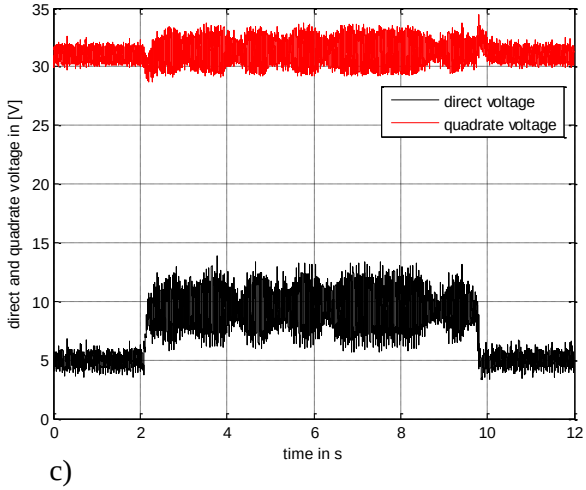

c)

Fig. 15. Experimental results under PI controller with charge: a) I_d and I_q measured currents, b), measured speed, c) quadrate and direct voltages

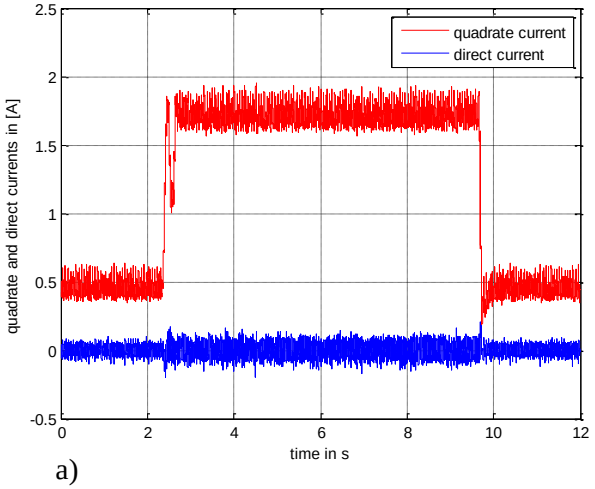

a)

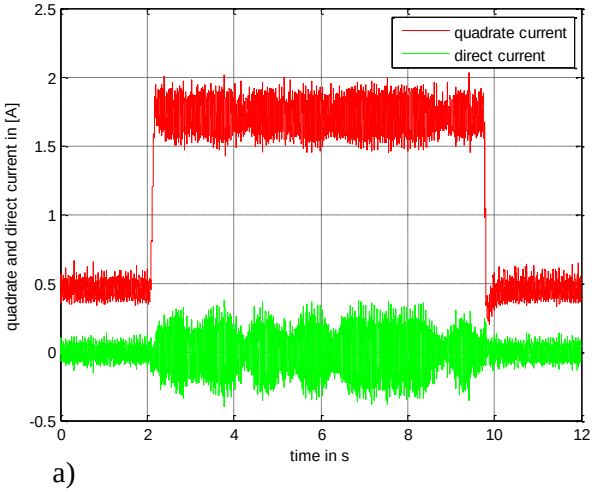

a)

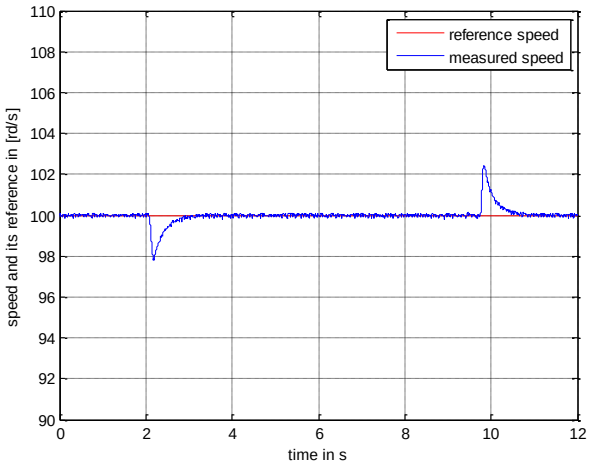

b)

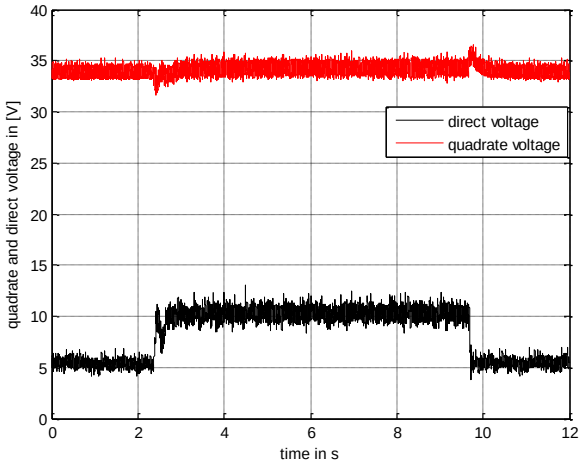

c)

Fig. 16. Experimental results under monovariable H_∞ controller with charge: a) I_d and I_q measured currents, b) measured speed
c) quadrate and direct voltages

Figures (14), (15) show results of stator currents, speed and dq voltages without and with charge under a PI controller. These results are satisfactory in terms of trajectory tracking and disturbance rejection. They are characterized by an overshoot of 5%, but the major disadvantage is that, in the transitory regime of speed response, there are oscillations which can induce some problems in some applications.

In comparison with results shown in Figures (9) and (16) we can derive that the monovariable H_∞ controller shows its superiority compared to the PI controller in terms of response time, overshoot.

This superiority is shown also in Figure (9) e) compared to Figure (14) e) which illustrate the error between speed and its reference.

Table 2
Performance and time characteristics of the three controllers

	settling time(ms)	overshoot (%)	static error (%)	training gap (%)
monovariable H_∞ controller	77	1	0	5
multivariable H_∞ controller	165	2	0	15
PI controller	220	5	0	13

Acknowledgments

Autors wish to thank all the team Laboratory of automation and industrial computing in the National Engineering School of Poitiers French and the resarch Unit of Industrial Processes Control " UIPC" in the National Engineering School of Sfax Tunisia which supported this work.

5. CONCLUSIONS

In this paper, a robust monovariable and multivariable H_∞ controllers have been synthesized in the purpose to ensure robustness in regard to parameters variations and disturbance rejection. A comparison of the two controllers indicates the superiority of the monovariable H_∞ controller as mentioned in table 2. Indeed, this method has smallest settling time, lowest overshoot and training gap with respect to multivariable H_∞ controller. This controller has proven also its superiority also in regard to a PI control law.

References

[1] H.Liu, S.Li. "speed control for PMSM servo system using predictive functional control and extended state observer". IEEE Transactions on Industrial Electronics vol 59. N°2 pp 1171-1183, February 2012.

[2] F.F M. El Sousy. "hybrid H^∞ based wavelet-neural network tracking control for permanent magnet synchronous motor servo drives". IEEE Transactions on Industrial Electronics vol 57. N°9 pp 3157-3166, September 2010.

[3] P. Thamizhazhagan, S.Sutha "performance analysis of direct torque controlled PMSM drives using fuzzy logic", Journal of Electric Engineering (JEE) Vol 17,

N° 1 article 17.1.32, pp 1-6, March 2017 .

[4] P.M.Pelecezewski., W.Oberschelp., & U.K.Kunz, "optimal model-following control of a positioning drive system with a permanent-magnet synchronous motor". IEEE Proceeding Control Theory and Applications, Part-D, Vol 138 (3), pp 267-273, 1991.

[5] N.Matsui., & H.Ohashi, "DSP-based adaptative control of a brushless motor". IEEE Transactions on Industry Applications, Vol 28 (2), pp 448-454, 1992.

[6] E.Cerruto, A.Consoli, A.Racitti, & A.Testa, "a robust adaptative controller of PM motor drives in robotic applications". IEEE Transactions on Power Electronics, Vol 10 (1), pp 62-71, 1992.

[7] T.H.Liu & C.P.Cheng, "Controller design for a sensorless permanent magnet synchronous drives system". IEEE. Proceedings Electrical Power Applications Part B, Vol.140 (6), pp 368-378

[8] S.Wang, K. Zhoa, W.Wang, L. Sun, D.Li, "nonlinear speed control for PMSM using Mixed H_2/H_∞ state output feedback control ". 17 th international conference on electrical machines and systems (ICEMS) pp 539-543, October 2014.

[9] T.H. Liu, C.P.Cheng, "control design for sensorless permanent magnet synchronous drive system". IEE Proceedings-B Vol 140 N°6 pp 369-378, November 1993.

[10] D.W. Gu, P.H.Petkov, M.M Konstantinov, "Robust control design with Matlab, second edition Springer-Verlag pp 1-389,London 2005.

[11] S.A. Zulkifli, M.Z.Ahmad, "H_∞ speed control for permanent magnet synchronous motor". International conference on electrical devices, systems and applications (ICEDSA) pp 290-293, July 2011.

[12] A.Fahkharian, V.Azimi, "Robust mixed sensitivity H_∞ control for a class of MIMO uncertain nonlinear IPM synchronous motor via T-S fuzzy model". 17th International conference on methods & models in automation & robotics (MMAR) pp 546-551 August 2012.

[13] P.Minarech, P.Makys, J. Vittek "PI-Controllers Determination for Vector Control Motion". Departement of Power Electrical Systems. Faculty of Electrical Engineering, University of Zilina Slovakia.

[14] J. Khedri, M.Chaabane, M. Souissi "Robust Control of a Permanent Magnet Synchronous Machine (PMSM) Using Internal Model Control". Proceedings of the International Technology Management Conference, pp 11-17, Antalya Turkey 2015.